2 Rutherford Cable Tests

Quench tests were performed using Rutherford cables. We measured quench propagation velocities and investigated how the current distributions in the cables made of non-insulated strands were changed locally during the quench process. In the first half of this chapter, the apparatuses used in the tests are explained. The latter half of this chapter presents test results.

2.1 Apparatus

Cables used in practical accelerator magnets consist of 20-30 strands, and the critical current level of the cables is quite large. If these practical cables are used in the tests, the number of channels to be measured becomes quite large. In addition, we cannot perform the measurements in the region of critical current and field because of the field and current limitation of the test stand. Therefore, an eight-strand Rutherford cable whose critical current was degraded by heat treatment was used in the tests. The specifications of the strand and Rutherford cable are shown in Table 2.1 and Table 2.2.

The strand consists of NbTi and copper. The diameter of the strand is about 0.808 mm and the Cu/Sc ratio is about 1.2. The strands are plated with Sn-5%Ag so that the contact conditions between the strands do not change as a function of time. The critical current of the strand was degraded by a heat treatment at 400 °C for 3 hours. The critical currents before and after the heat treatment are shown in Fig. 2.1.

A Rutherford cable consists of 8 strands, and the twist pitch is about 31 mm. The cable is wrapped with 50% overlap by a polyimide tape of 5 mm in width and 20 μm in thickness. Thus the cable conditions are similar to those of cables used in practical magnets.

The schematic view of the experimental setup is shown in Fig. 2.2. In order to perform

a measurement in a magnetic field, the sample cable is arranged in a U-shape in the bore of a 1 m-model SSC dipole magnet [26]-[28]. The physical length of the magnet is about 1.5 m, the diameter of the bore is 5 cm, and the uniform field length is about 1 m. Measurements are performed using two regions under a uniform magnetic field, Region A and Region B in Fig. 2.2. The sample holder consists of parts of GFRP and stainless steel. The cross section of the sample holder is shown in Fig. 2.3. The cable is sandwiched by GFRP parts with an average pressure of 15 MPa, which is controlled by the torque of bolts. The length of the sample cable is about 3.6 m. At the ends of the cable, the cable is un-twisted and separated individually. Then, the strands of both ends are soldered on copper plates. The whole sample is vertically mounted in a 2.8 m long vertical cryostat and cooled at 4.2 K with pool boiling liquid helium. Fig. 2.4 shows the overview of the sample in the cryostat.

Experimental devices for measurements of quench processes are attached to the cable. They are heaters, voltage taps and sets of pickup coils. The positions of the devices placed in the measurement regions are shown in Fig. 2.5. The numbers in parentheses are the relative positions of the devices with respect to VTA or VTN.

Carbon paste heaters [29, 30] are attached to the cable to initiate quenches. In order to apply a heat pulse to a single strand, a heater is attached as shown in Fig. 2.6. The length of the heater is about 1.5 mm, and it is covered with epoxy for thermal insulation from liquid helium. The resistance of the heater is 1-100 Ω depending on the heater position.

The voltage taps are attached to each strand in order to observe the quench propagation.

The details of the arrangement of pickup coils are described in the next section.

2.2 Pickup Coil

2.2.1 Theory

In the present study, the transient and local current redistributions in the cable made of non-insulated strands were measured with pickup coils. Another technique for measurements of local current redistributions is the one using Hall sensors [31, 32]. This technique also enables us to measure the static current distribution. However, for the measurement of the cable exposed to an external magnetic field, the technique using pickup coils is much reliable, since the offset voltages of Hall sensors due to an external magnetic field disturb precise measurements.

The schematic view of pickup coils used in the present study is shown in Fig. 2.7. The parameters of the pickup coil are listed in Table 2.3. The eight rectangular coils are arranged around the eight-strand Rutherford cable. The coil width and length are 1.2 mm and 2.2 mm, respectively. The copper wire of 50 μm in diameter was wound on GFRP fixtures, and the number of coil windings was 15 turns. A photograph of the pickup coil parts is shown in Fig. 2.8. One set of the pickup coils consists of two GFRP fixtures, in which the sample cable is fixed.

The amount of current changes is determined from the change of local magnetic field around the strand. The induced voltages of pickup coils are written as

$$\begin{pmatrix} v_1 \\ \vdots \\ v_8 \end{pmatrix} = \begin{pmatrix} m_{11} \ldots m_{18} \\ \vdots \ \ddots \ \vdots \\ m_{81} \ldots m_{88} \end{pmatrix} \begin{pmatrix} di_1/dt \\ \vdots \\ di_8/dt \end{pmatrix} \equiv \boldsymbol{V} = \boldsymbol{M}\dot{\boldsymbol{I}} \tag{2.1}$$

where $\boldsymbol{V}(v_1, \ldots, v_8)$ is the induced voltage of a pickup coil, $\boldsymbol{I}(i_1, \ldots, i_8)$ is the strand current, and m_{ij} is the mutual inductance between the pickup coil and strand, and i and j represent the coil index and the strand index, respectively. The above equation can be rewritten as

$$\Delta \boldsymbol{I} = M^{-1} \int \boldsymbol{V} dt \equiv \begin{pmatrix} \Delta i_1 \\ \vdots \\ \Delta i_8 \end{pmatrix} = \begin{pmatrix} m_{11} \ldots m_{18} \\ \vdots \ \ddots \ \vdots \\ m_{81} \ldots m_{88} \end{pmatrix}^{-1} \begin{pmatrix} \int v_1 dt \\ \vdots \\ \int v_8 dt \end{pmatrix} \tag{2.2}$$

Therefore, we can calculate the current changes of each strand from the output voltages of the pickup coils.

2.2.2 Determination of the Coil Size and Arrangement

In order to solve Eq. (2.2), the matrix M must not be a singular matrix. An ideal matrix to measure the local current changes of each strand with high accuracy is that all values in matrix are zero except for the values on the diagonal. This can be satisfied when a coil is only sensitive to the current change of the nearest strand. In practice, since the mutual inductance matrix M is determined by the size and arrangement of the pickup coils, it is necessary to examine these parameters.

Let us consider the coil length. For the cable used in the tests, the sensitive length of the coil in the longitudinal direction must be shorter than 3.875 mm, which corresponds to about one-eighth of the cable twist pitch of 31 mm. If the sensitive length is longer than 3.875 mm, a coil becomes sensitive to the current change of neighboring strands. This eventually increases singularity of the matrix M, and decreases the measurement accuracy. In order to examine whether the coil length of 2.2 mm is sufficiently short, we calculated the flux across the coil made by a current piece. Fig. 2.9 shows the calculated flux. The configuration of the calculation is illustrated on the right-top of the figure. The current piece with 10 A and 0.5 mm in length is placed along the line drawn apart by 1.21 mm from the coil center. The distance of 1.21 mm corresponds to the distance between the coil center and the cable center. The horizontal axis is the longitudinal position of the current piece and the vertical axis is the flux of the coil. As shown in this figure, the flux of the coil decreases gradually with increasing distance x. The flux at x=4 mm is about 3 % of the peak flux at x=0 mm. Namely, the sensitive length of the coil is shorter than 3.875 mm, and it is found that the coil length of 2 mm is short enough to neglect the decrease of the measurement accuracy due to the twist of the cable.

Next, the arrangement of the pickup coils is examined. Two arrangements of the coils are considered as shown in Fig. 2.10. In type-A, all the coils are parallel to each

other (Fig. 2.10(a)), and in type-B, all the coils have certain angles (Fig. 2.10(b)). Type-A is the arrangement used in the present study. In the two arrangements, we calculated the mutual inductances between the coils and strands. Fig. 2.11 shows the normalized mutual inductances between each coil and strand 1. The vertical axis is the mutual inductance normalized by the maximum mutual inductance. The closed and open circle symbols show the calculated values of type-A and type-B, respectively. The closed square symbols represent the values so that the linearity of the matrix M is the highest. Since it can be seen from this figure that type-A is slightly better than type-B, it is reasonable to use the type-A pickup coil set.

2.2.3 Calibration

In the present study, the mutual inductances were obtained experimentally. This experiment is called a *calibration test*, and the calibration test was performed at room temperature. Advantages of this procedure are to reduce the uncertainties caused by errors of relative positions in the longitudinal direction between the set of pickup coils and the cross section of the cable and by errors in coil size or shape.

A *dummy cable* was used in the calibration test. It was identical to the actual Rutherford cable (Table 2.2) except that the strands were insulated. The procedure of the calibration test is as follows:

1. the sets of pickup coils are attached to the dummy cable to be in the same position as in the test with liquid helium,
2. an alternating current is flowed in one strand,
3. the induced voltages of the pickup coils are measured,
4. these voltages are compared with the amplitude of the current, and
5. the strand is changed, and procedures 2-4 are repeated.

Fig. 2.12 shows an example of the induced voltages of the pickup coils in the calibration test, where the current with an amplitude of 4.6 A and frequency of 512.5 Hz flowed in strand 8. The illustration on the right-bottom in this figure represents the arrangement

of the pickup coils and the cable.

When the mutual inductances were obtained experimentally like this, we must note the accuracy of the attachment of the pickup coil set. If the position of the pickup coil set in the test with liquid helium is different from the position in the calibration test, the measurement accuracy decreases. Therefore, we examined the repeatability of the attachment of the pickup coil set using the dummy cable. First, the mutual inductance matrix was obtained by the calibration test. Next, the pickup coil set was detached and attached once more so that the position of the pickup coil was the same as that in the calibration test. The current with 10 $A_{peak-to-peak}$ and 512.5 Hz was flowed in strand 1, and the coil voltages were measured. The procedures after detaching the pickup coil set were repeated ten times, and the each strand current was calculated at every test using the inductance matrix obtained beforehand. This result is shown in Fig. 2.13. Fig. 2.13(a) shows the calculated peak-to-peak current of each strand at each measurement. As can be seen from this figure, at every measurement, the currents of strand 1 are almost 10 $A_{peak-to-peak}$, and the currents of the other strands are less than 0.4 A. Fig. 2.13(b) shows the calculated current of strand 1 normalized by the actual current flows in strand 1. Through the ten times measurements, the error of the calculated current is less than 5%. Since the calculated current at every measurement is almost the same, it seems that the accuracy of the attachment of the pickup coil set is sufficiently good.

2.3 Test Results

Two heater quench tests were performed under four cable conditions as follows: (a) a cable with no treatment, (b) a cable stripped of polyimide tape for cable insulation, (c) a cable with lower electrical contact conductance and contact thermal conductivity between strands, and (d) a cable with higher electrical contact conductance and contact thermal conductivity between strands. The cables having the above conditions are called *original* cable, cable *without polyimide*, *low contact* cable and *high contact* cable, respectively. For low contact cable, after the cable was un-twisted and separated from each other, a heat treatment at 180 °C for 4 hours was applied to the cable. For high contact cable, the cable was impregnated with solder. The changes of contact conditions were examined by measuring electrical contact conductance between neighboring strands [33]. For original cable, low contact cable and high contact cable, the conductance between strands were 2.5×10^{7} S/m, 2.5×10^{5} S/m and 2.5×10^{10} S/m, respectively. Table 2.4 summarizes the cable conditions of the two measurement regions in each test.

The procedure of heater quench tests is as follows:

1. the magnet is excited up to 4 T,
2. current is supplied to the cable, and kept for one minute,
3. a heat pulse with a time duration of 1 msec is applied to a strand by the carbon paste heater, and a quench is initiated, and
4. during the quench propagation process, signals of sensors are measured by an A-D converter and stored in a work station.

Signals of the voltage taps and pickup coils were amplified by isolation and differential amplifiers, respectively. We designed and fabricated simple differential amplifiers. The details of these amplifiers will be given in Appendix A. The sampling frequency of the A-D converter was 25600 Hz.

2.3.1 Quench Propagation Velocity

First, the results of quench propagation velocities are explained. An example of the longitudinal quench propagation of the cable is shown in Fig. 2.14, where the cable current was about 3100 A, and the quench heater used in the tests was HTB attached to strand 5. The quench was initiated at 0 msec. The signals in this figure represent the voltages between voltage taps attached to strand 5. We can see from this figure that the voltages between each pair of voltage taps appeared as the quench propagated. The quench propagation velocity was derived by dividing the distance between two voltage taps by the difference of the take-off times between the voltage tap signals.

Figure 2.15 shows the average quench propagation velocity for the four cable conditions as a function of cable current. The vertical axis is the average of the velocities measured at four sections: VTB-VTC, VTC-VTD, VTD-VTE and VTE-VTF in Region A, or VTI-VTJ, VTJ-VTK, VTK-VTL and VTL-VTM in Region B. (See Fig. 2.5.) Each symbol represents the average velocities for the four cable conditions, and error bars represent the amounts of spreads in the velocities at each section. The heaters used were HTB and HTC.

We discuss first the influence of the polyimide tape for cable insulation on the quench propagation velocity. From Fig. 2.15, in cable without polyimide, there was little spread of the velocities at every cable current, namely, the velocities were almost the same for the four sections. On the contrary, in original cable, there was a large spread of the velocities and the spread increased continuously in the cable current range above about 2900 A. Fig. 2.16 shows the velocities of original cable at the four sections, where the cable current was 3100 A. The closed circles represent the velocity when heater HTA was used, and the open circles represent the velocity when heater HTB was used. It can be seen from this figure that the velocities depend on the positions, regardless of the direction of quench propagation. This dependence was almost the same as in low contact cable and high contact cable.

Next, let us consider the influence of contact conditions between strands. The velocities of low contact cable were generally lower than those of the other two conditions.

For original cable and high contact cable, the average velocities were almost the same in the current range below 3000 A. In the current range more than 3000 A, the average velocities of original cable were higher than those of high contact cable.

2.3.2 Current Redistribution

Figures 2.17 - 2.20 show examples of eight pickup coil signals for the four cable conditions. The cable currents were 3100 A for all the cables, and the quench heaters used were HTA, HTC, HTB and HTD for original cable, cable without polyimide, low contact cable and high contact cable, respectively. The indexes of pickup coils were assigned to the number of the nearest strand. For all the cables, the time of clear pulses appearing in each figure corresponds to the time when the *quench front*, which is the boundary between the superconducting state and the normal state, passed through the positions of pickup coil sets. It can be seen that in the cable made of non-insulated strands, the current redistribution occurred mainly around the quench front.

Let us analyze the details observed in original cable. Two clear pulses appeared when the quench front passed. And the second pulse had the opposite polarity of the first pulse. In cable without polyimide, the shapes of signals were quite similar to those in original cable, while the pulse heights were generally smaller. In low contact cable, there were some oscillating pulses, and the time span that the signals appeared was longer than those in the other conditions. This fact indicates that the region of the redistribution in low contact cable is wider than those in the other conditions. On the contrary, in high contact cable, only a single pulse appeared at the time when the quench front passed.

Using Eq. (2.2), the current changes of each strand were calculated. Fig. 2.21 shows the current changes of each strand calculated from the signals in Fig. 2.17. Each symbol represents the current change of each strand. The illustration on the left-bottom shows the strand positions at the position of the pickup coil set. In original cable, for example, the current of strand 1 increased greatly when the quench front passed, and then the current somewhat decreased. On the contrary, the current of strand 4 decreased first,

and then it increased slightly. With respect to the strand positions, the first current redistribution occurred from the left side to the right side of the cable, and the second current redistribution occurred from right to left. Such a current redistribution can be explained by taking the magnetic field distribution into account. As shown in Fig. 2.22, the cable was exposed not only to the external magnetic field produced by the magnet but also to the magnetic field produced by itself. Therefore, a magnetic field gradient was produced across the cable cross section.

The maximum and minimum magnetic fields on the cable cross section were estimated. In Fig. 2.22, the strands exposed to the maximum and minimum fields are the two strands in the left and right sides, respectively. In the Rutherford cable tests, the critical current of the cable which was measured before the heater quench tests was about 3200 A at 4 T in all the four cables. Considering the current flows in the strands as the line current. When the strand current is 400 A, the self magnetic field at the strands in the left and right sides is about 0.3 T in the direction of the external magnetic field . Therefore, the maximum and minimum fields, B_{max} and B_{min}, at the external magnetic field of 4 T are given by

$$B_{max}[\mathrm{T}] = 4.0 + 0.3 \times \frac{I_{strand}}{400}, \tag{2.3}$$

$$B_{min}[\mathrm{T}] = 4.0 - 0.3 \times \frac{I_{strand}}{400}, \tag{2.4}$$

where I_{starnd} is the average current of one strand in amperes. At the cable current of 3100 A (I_{starnd} = 387.5 A), the maximum difference of the magnetic fields reaches to about 0.58 T.

In the case of the cable with the field distribution as shown in Fig 2.22, the higher field region of the cable becomes the normal state first, when the normal zone reaches. Then the current moves to the lower field region of the cable. After the lower field region becomes the normal state due to the increased current and due to the thermal conduction through a strand, the surplus current returns to the higher field region in order to make the current distribution over the cable cross section even.

Figure 2.23 shows the current changes of each strand at the time, t_{fcr}, when the first current redistribution occurred. Precisely, t_{fcr} was defined as the time when the average

current change was maximum as shown in Fig. 2.24(a). As can be seen in Fig. 2.23, with increasing cable current, the more current moved from the left side to the right side. The reason for this effect was considered to be due to the fact that the field gradient on the cable became steep.

Figure 2.25 shows the first current redistribution at some longitudinal positions in original cable. The amount of current changes is distinguished by colors. The pictures on the left side row are the data for the cable current of 2600 A, and the pictures on the right side row are the data for the cable current of 3100 A. As can be seen in this figure, with increasing cable current, the first current redistribution occurred from the high field region to the low field region everywhere in the longitudinal direction.

Figures 2.26-2.28 show the current changes of cable without polyimide. The signal shapes were similar to those in original cable shown in Fig. 2.21. While the current redistribution was not influenced by the magnetic field distribution, as can be seen in Fig. 2.27. The reason for this is considered that the cooling effect of liquid helium becomes large due to the absence of polyimide tape. This effect seems to overwhelm the influence of magnetic field distribution.

In low contact cable, we can see from Fig. 2.29 that the currents of all strands oscillated up and down around the quench front, and the time span of the current change was slightly longer than that in original cable. And there was little influence of the magnetic field distribution on the current redistribution as in cable without polyimide (Figs. 2.30 and 2.31). The reason seems to be due to the fact that the current redistribution cannot occur within a short distance in low contact cable.

Figures 2.32-2.34 show the current changes of high contact cable. As can be seen in Fig. 2.32, the current moves only from the high field region to the low field region. At any cable current, this tendency appeared clearly, and there was no dependence on longitudinal positions.

Table 2.1: Specifications of the strand.

Diameter	0.810 mm
Superconductor	NbTi
Matrix	Copper
Residual Resistivity Ratio (RRR)	91
Copper / Superconductor Ratio	1.2
Surface	Sn-5%Ag (Staybrite) plated
Critical Current	586 A at 3 T
	435 A at 4 T
	324 A at 5 T

Table 2.2: Specifications of the Rutherford cable used in the tests.

Number of Strands	8
Width	3.30 mm
Thickness	1.53 mm
Twist Pitch	31 mm
Twist Direction	S
Cable Insulation	
Material	Polyimide
Width	5 mm
Thickness	25 μm
Wrapping Direction	Z
Way of Wrapping	50% overlap

Table 2.3: Specifications of the pickup coil.

Length	2.2 mm
Width	1.2 mm
Turn Number	15
Coil Wire	Copper Wire with ϕ 50 μm

Table 2.4: Cable conditions of Region A and Region B.

Test Name	Condition of Region A	Condition of Region B
#001	Original[a] (2.5×10^{7} S/m)	Without polyimide[b] (2.5×10^{7} S/m)
#002	Low contact[c] (2.5×10^{5} S/m)	High contact[d] (2.5×10^{10} S/m)

Values in parentheses are electrical contact conductance between neighboring strands.

[a]Cable with no treatment.

[b]Cable stripped of polyimide tape for cable insulation.

[c]Cable with lower electrical contact conductance and contact thermal conductivity between strands.

[d]Cable with higher electrical contact conductance and contact thermal conductivity between strands.

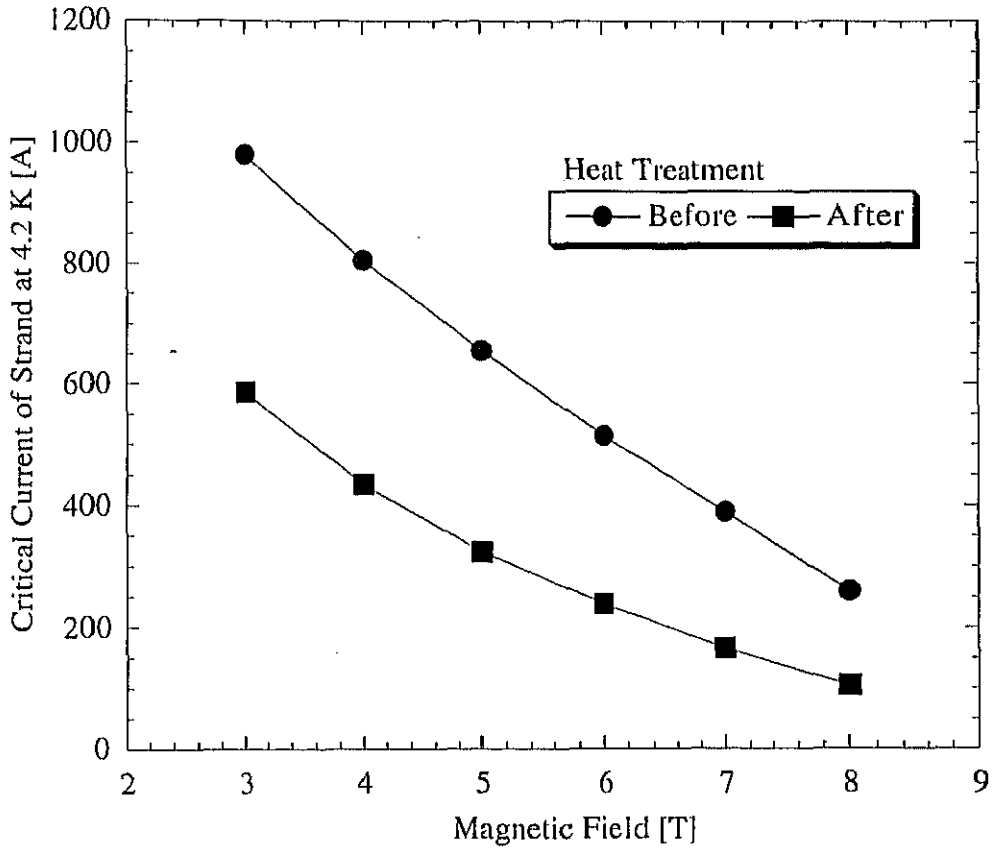

Fig. 2.1: Critical current of the short strand before and after the heat treatment.

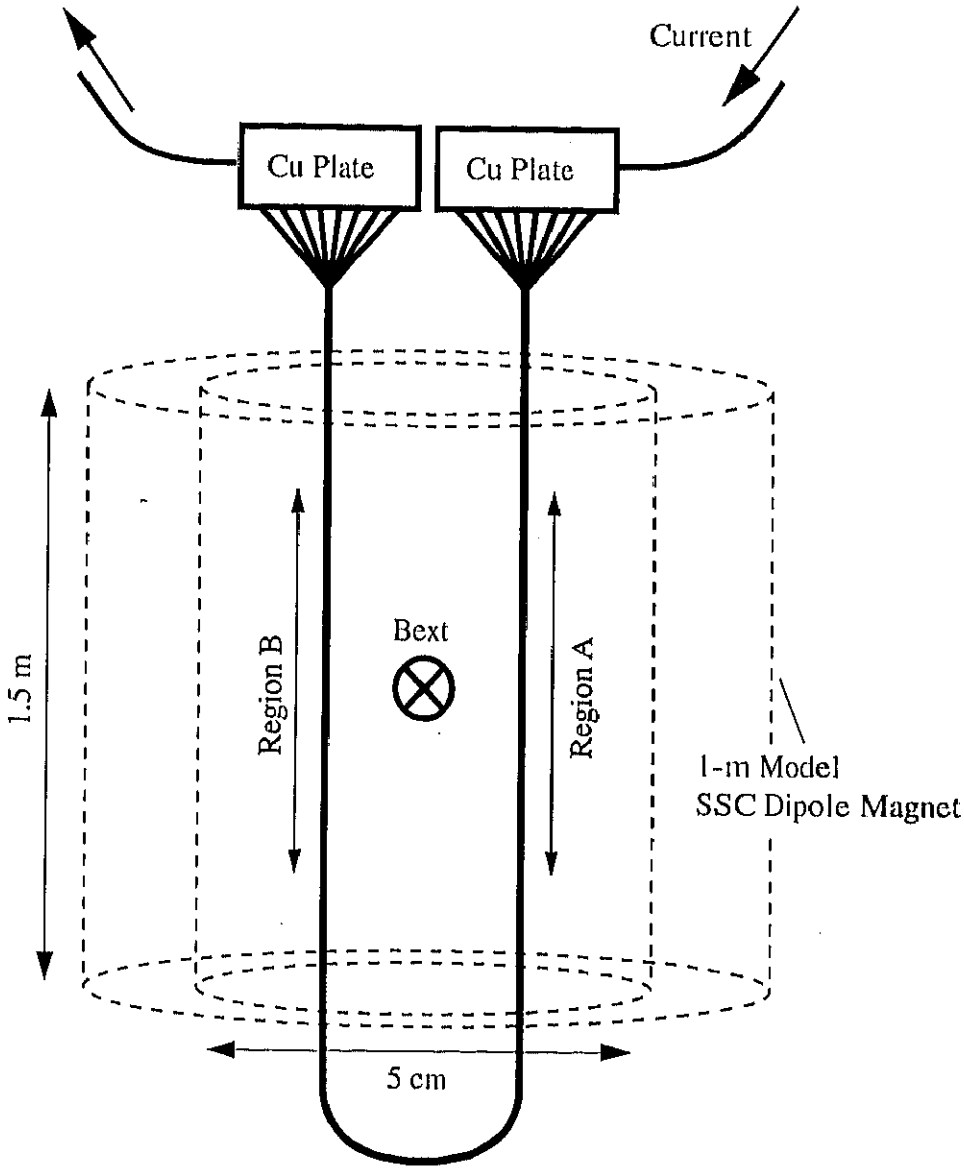

Fig. 2.2: Schematic view of the sample cable and the dipole magnet.

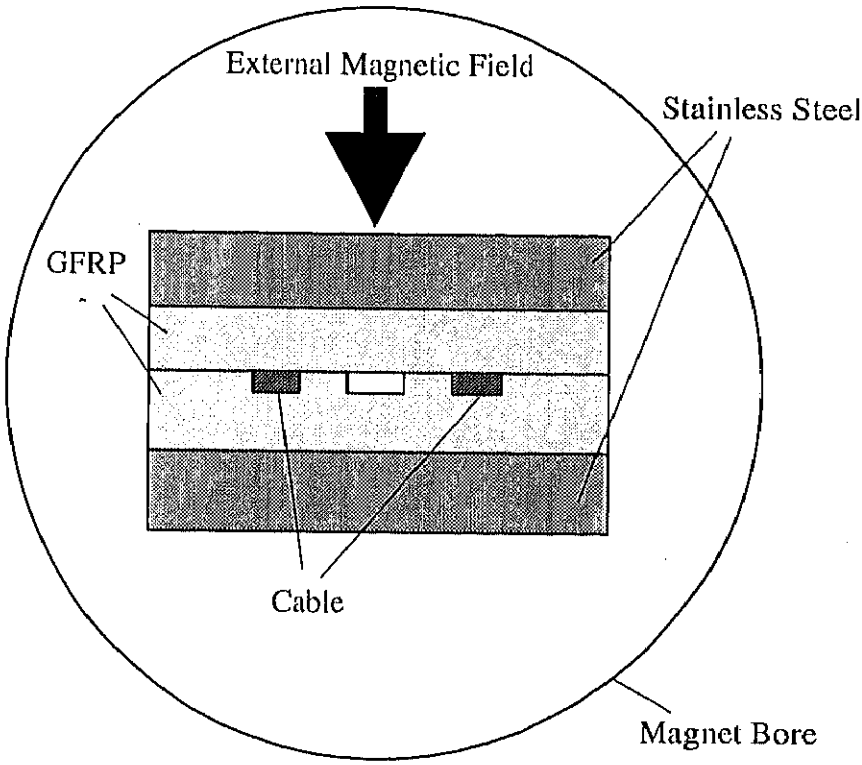

Fig. 2.3: Cross section of the sample holder.

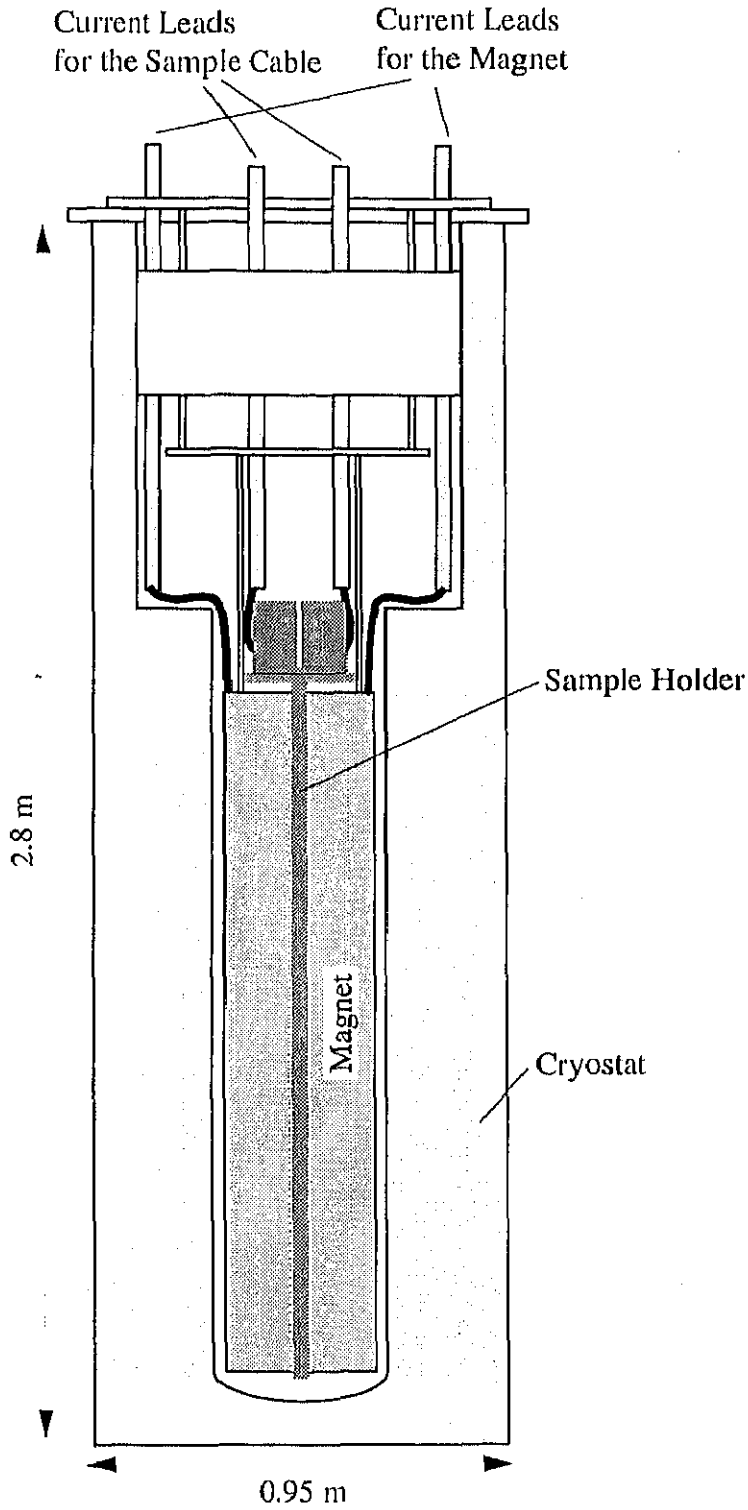

Fig. 2.4: Overview of the experimental setup.

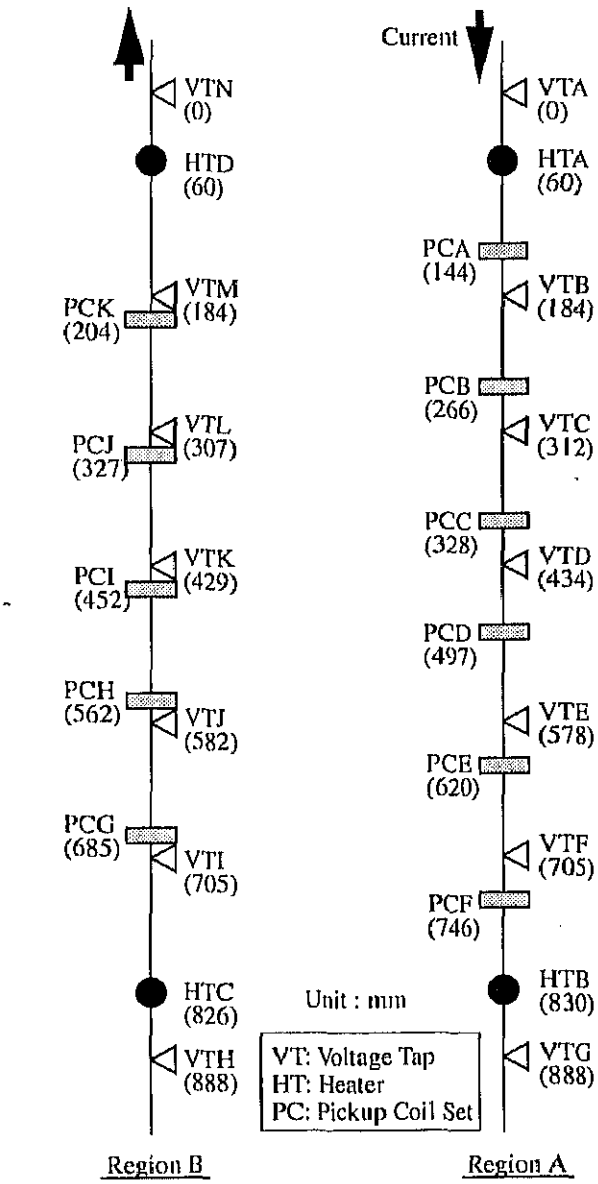

Fig. 2.5: Positions of the heaters, the voltage taps and the set of pickup coils. VT, HT and PC represent the voltage taps, the carbon paste heater, and the set of pickup coils. The numbers in parentheses are the relative positions of the devices with respect to VTA or VTN.

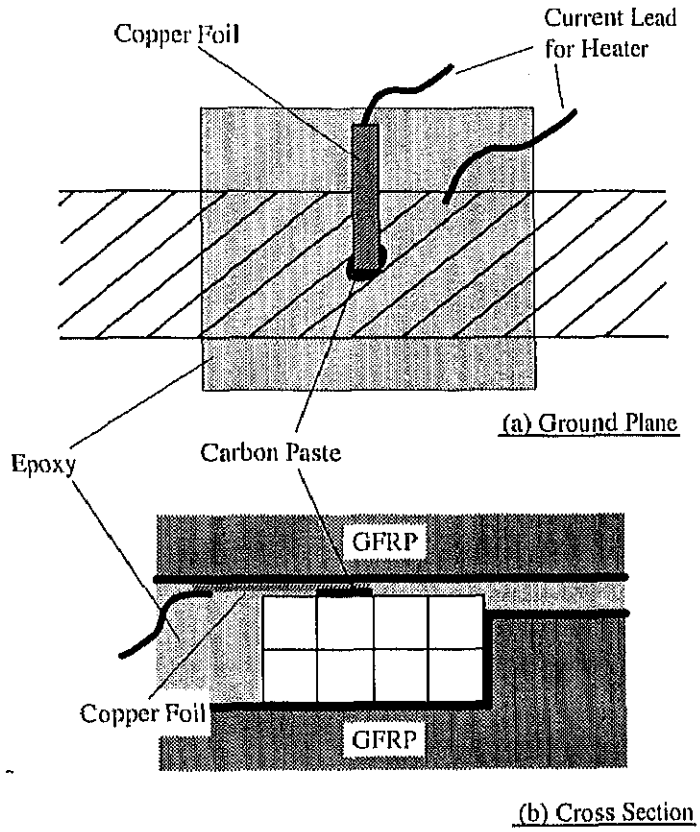

Fig. 2.6: Schematic view of the carbon paste heater.

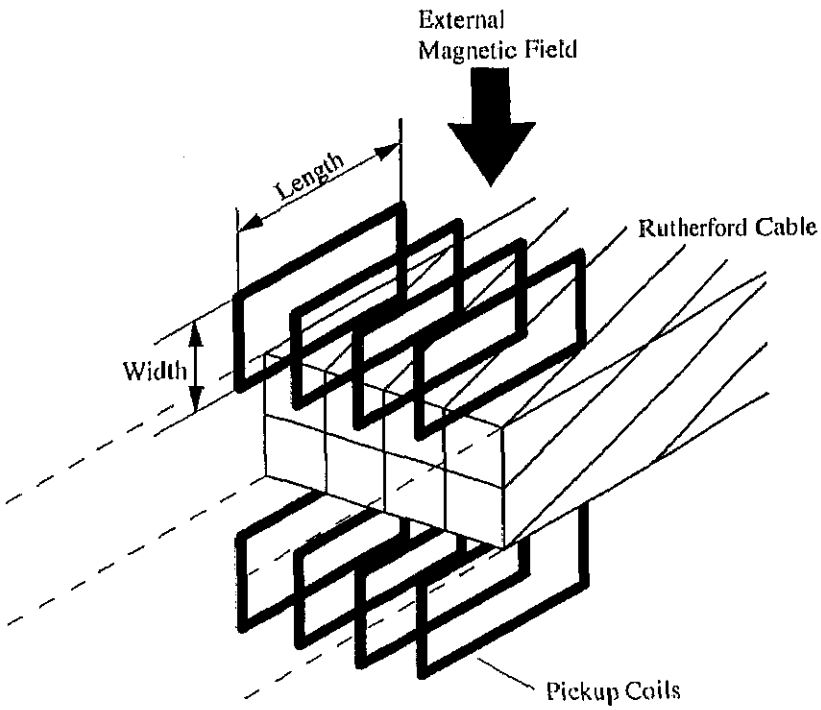

Fig. 2.7: Schematic view of pickup coils.

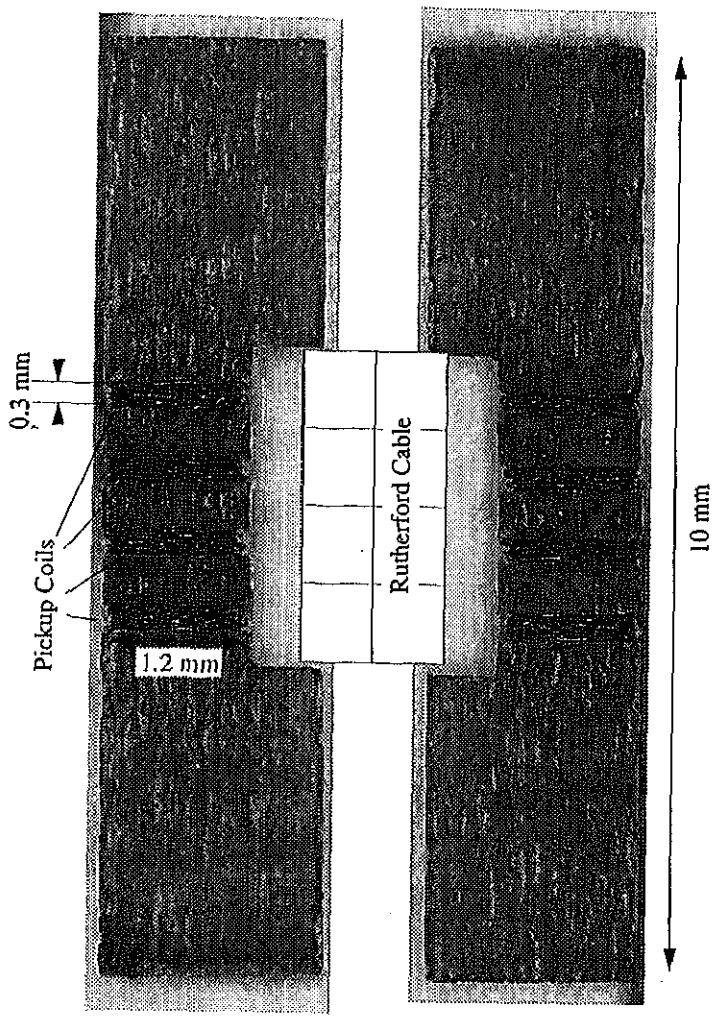

Fig. 2.8: Photograph of pickup coils with GFRP fixtures.

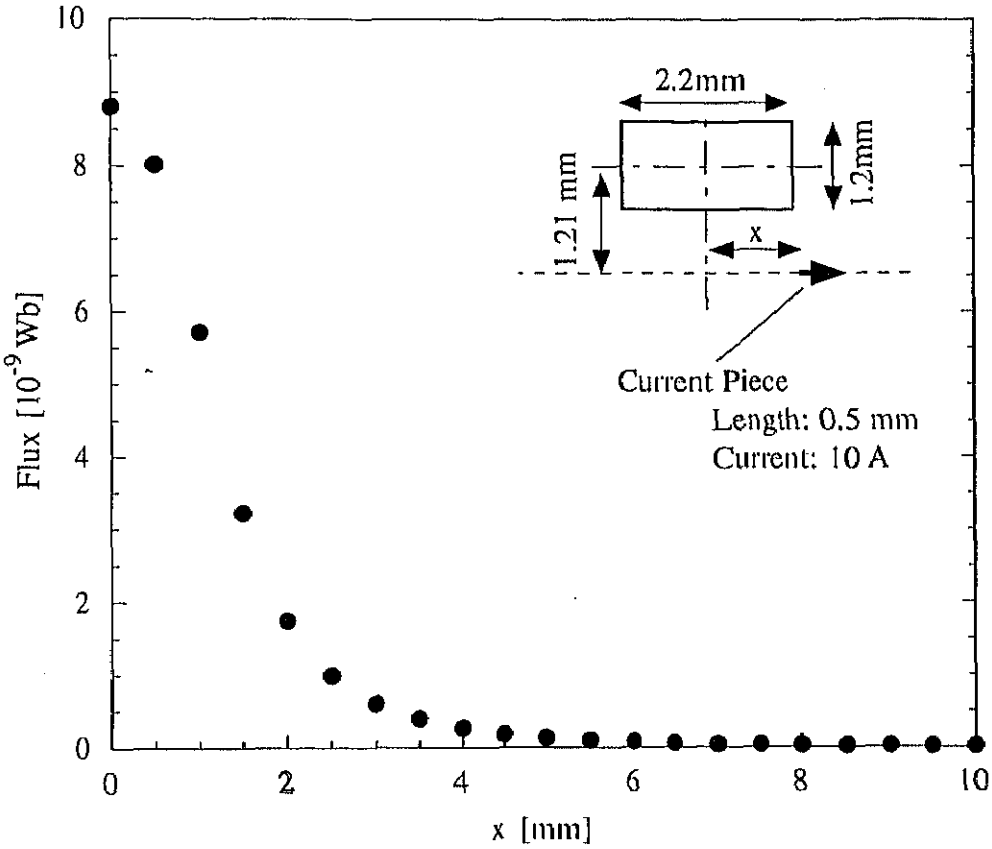

Fig. 2.9: Calculated flux across the coil made by a current piece. The illustration on the right-top represents the configuration for the calculation.

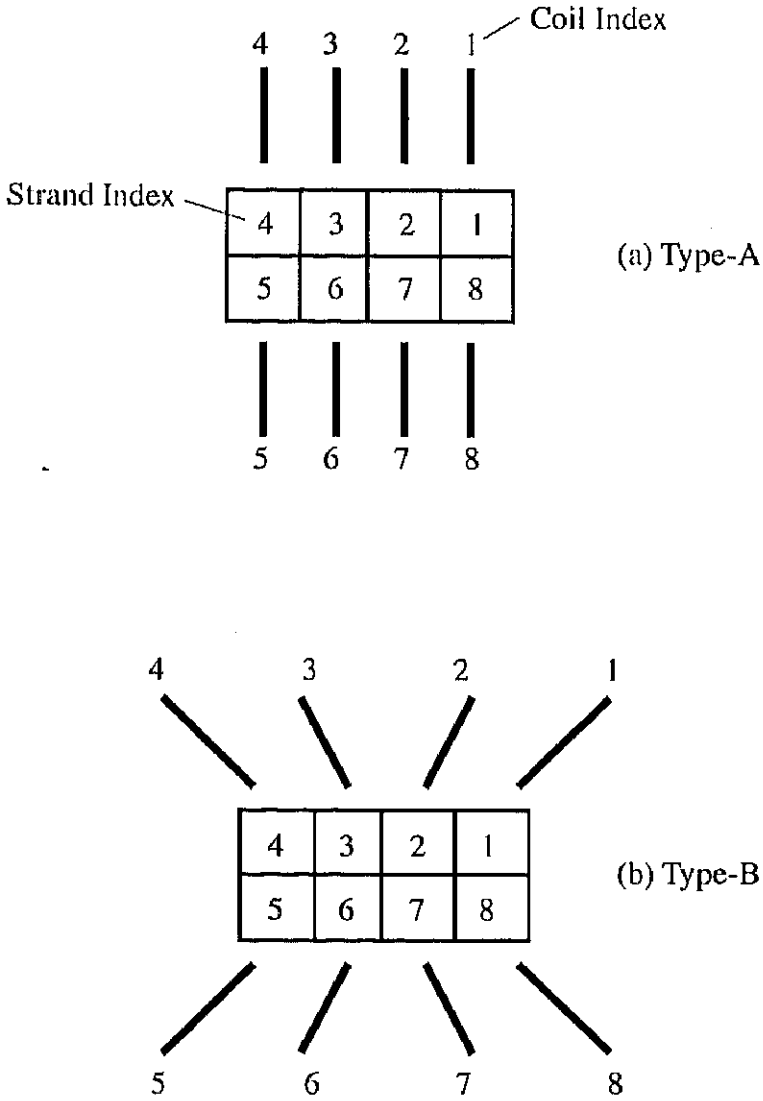

Fig. 2.10: Two types of coil arrangements. Type-A is the arrangement used in the present study.

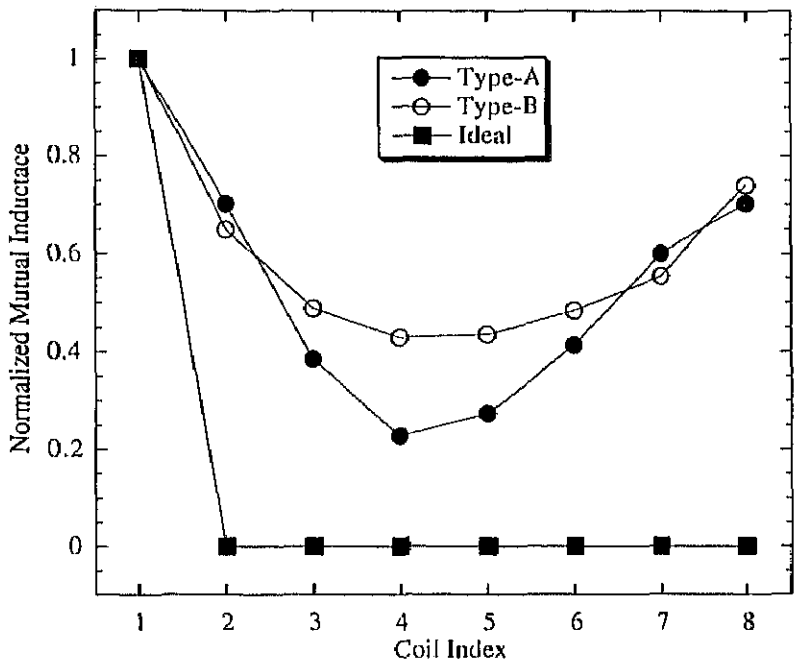

Fig. 2.11: Calculated mutual inductance normalized by the maximum inductance.

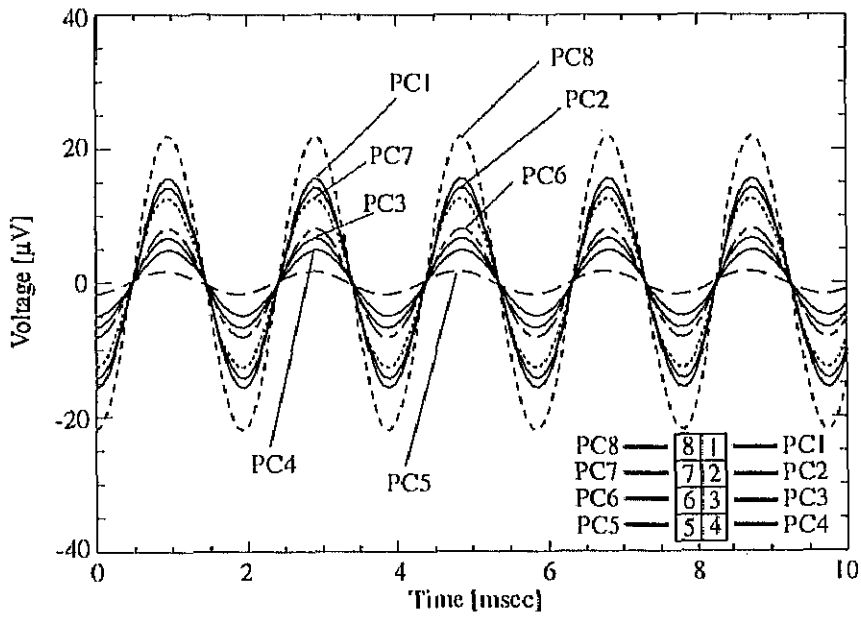

Fig. 2.12: Example of the induced voltages of the pickup coils in the calibration test, where the current with amplitude of 4.6 A and frequency of 512.5 Hz flowed in strand 8.

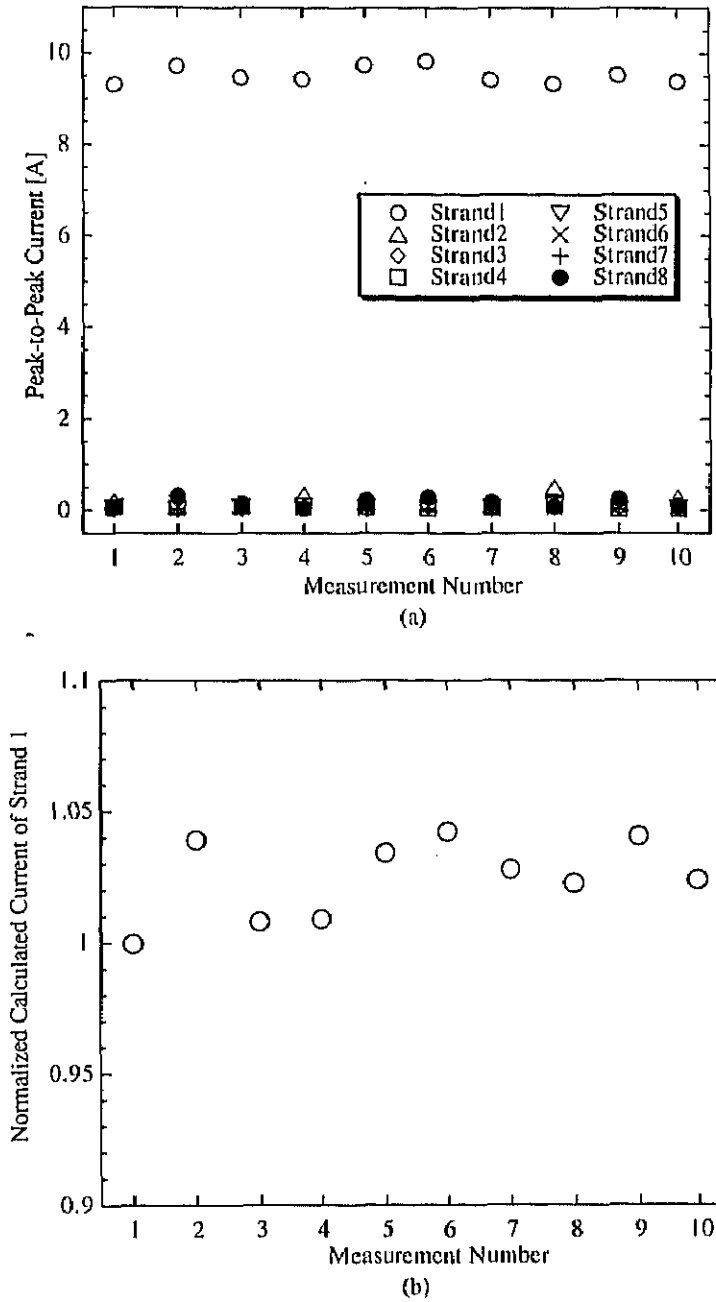

Fig. 2.13: Repeatability of the attachment of the pickup coil set. The current of 10 $A_{peak-to-peak}$ flows through only strand 1. (a) shows the calculated current of each strand. (b) shows the calculated current of strand 1 normalized by the actual current flows in strand 1.

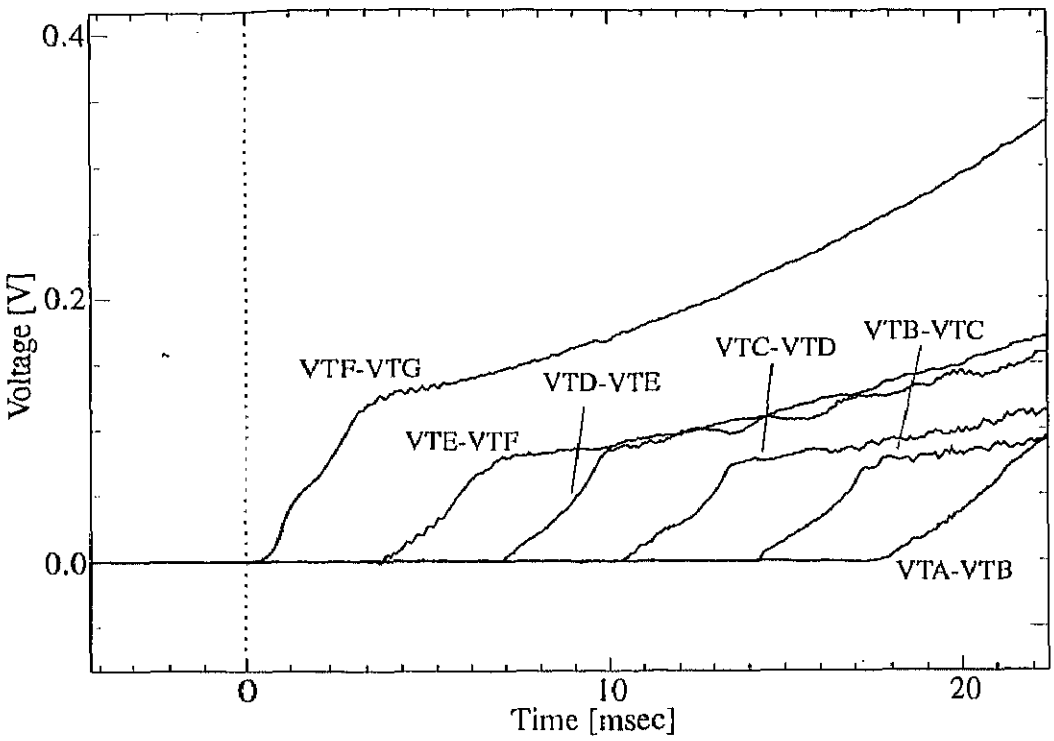

Fig. 2.14: Example of the longitudinal quench propagation of the cable for the cable current of about 3100 A. Quench heater HTB was attached to strand 5. The quench was initiated at 0 msec. The signals represent the voltages between voltage taps attached to strand 5.

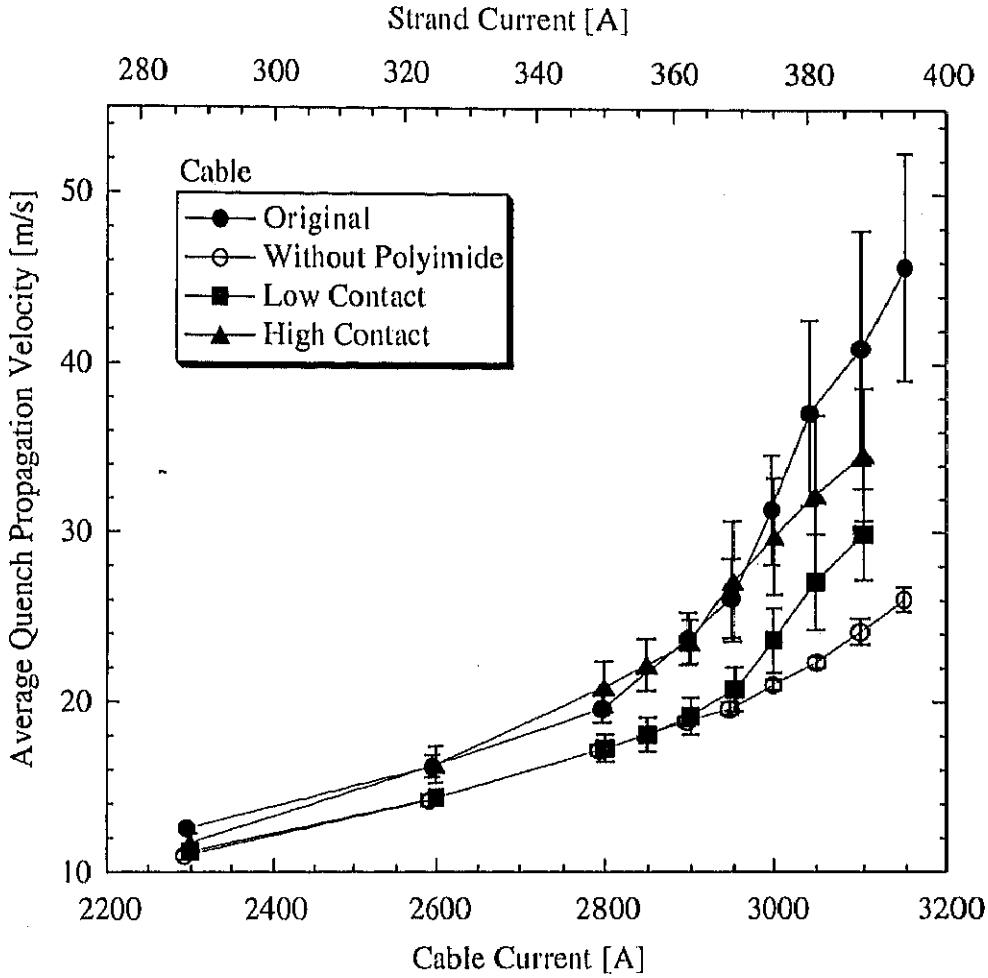

Fig. 2.15: Average quench propagation velocities for the four cable conditions as a function of cable current. The error bars represent the amounts of spreads in the velocities at each section. The heaters used were HTB for original cable and low contact cable, and HTC for cable without polyimide and high contact cable.

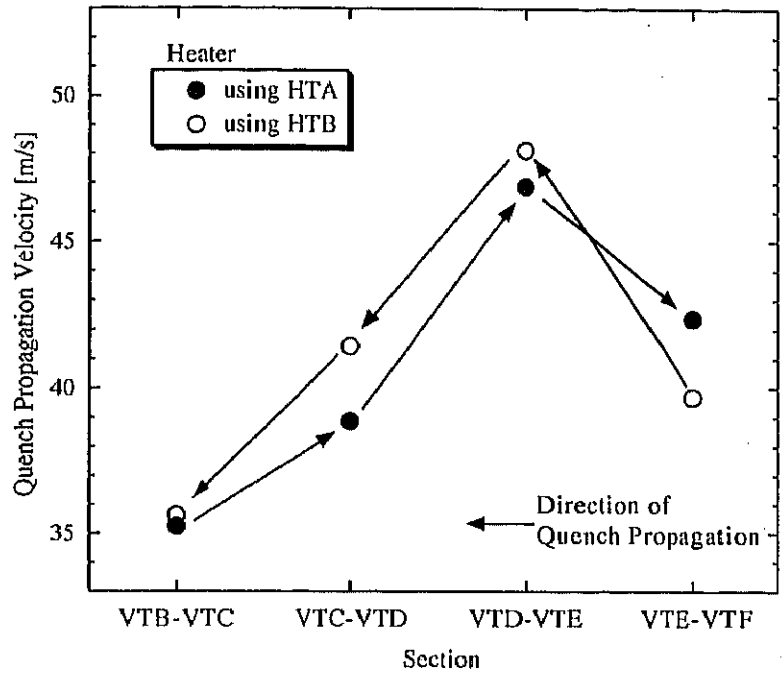

Fig. 2.16: Quench propagation velocities of original cable at the four sections with the cable current of 3100 A.

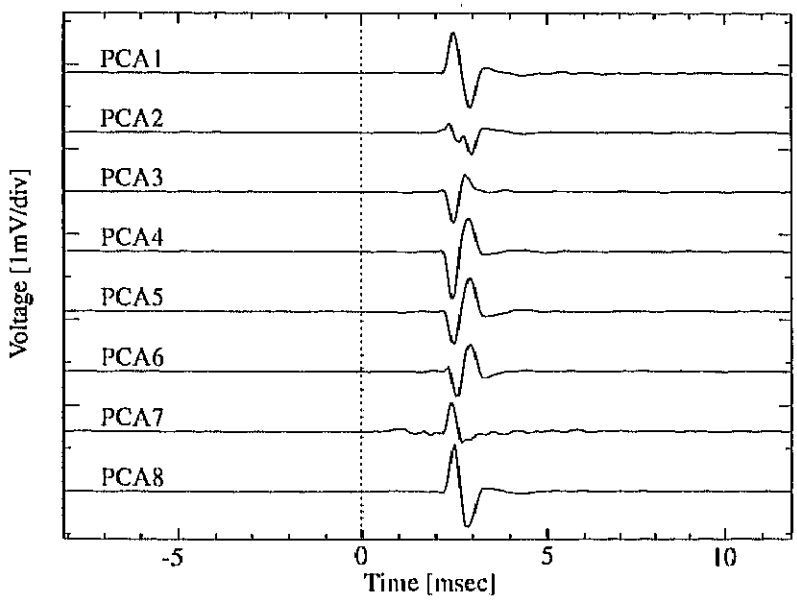

Fig. 2.17: Example of the pickup coil signals in original cable. The cable current was about 3100 A, and the quench heater used was HTA.

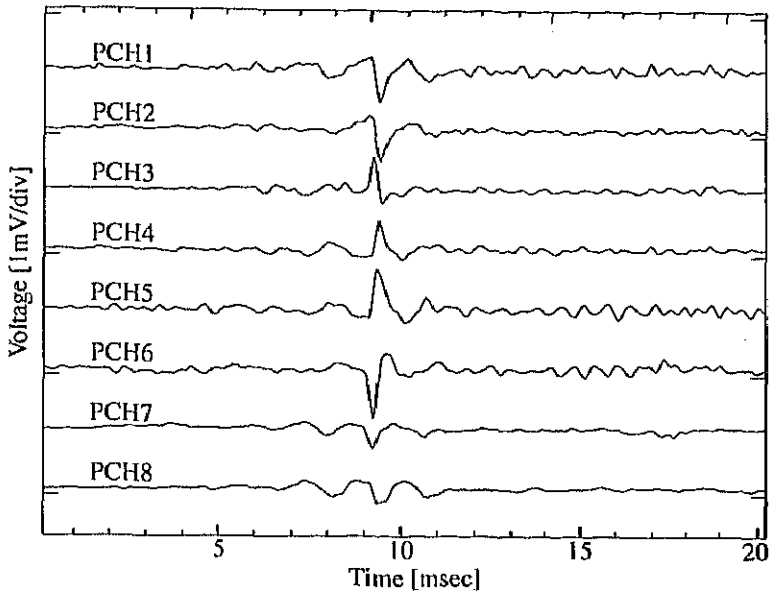

Fig. 2.18: Example of the pickup coil signals in cable without polyimide. The cable current was about 3100 A, and the quench heater used was HTC.

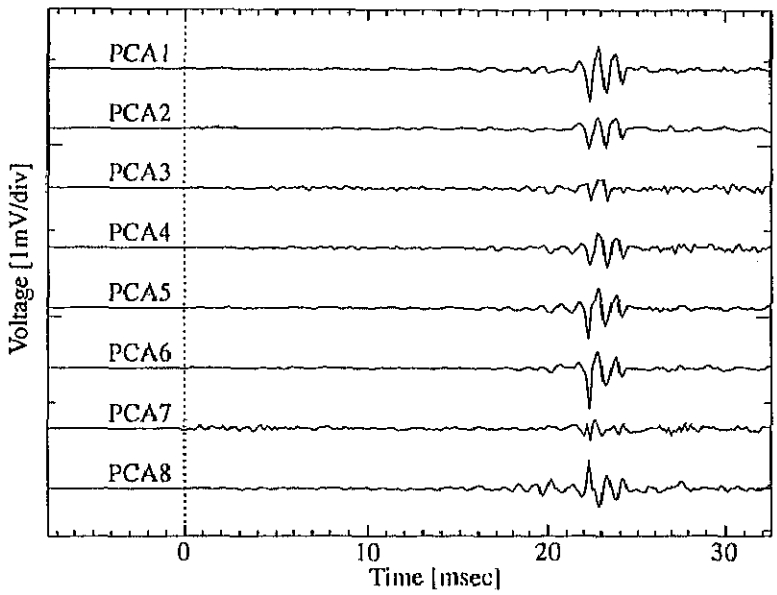

Fig. 2.19: Example of the pickup coil signals in low contact cable. The cable current was about 3100 A, and the quench heater used was HTB.

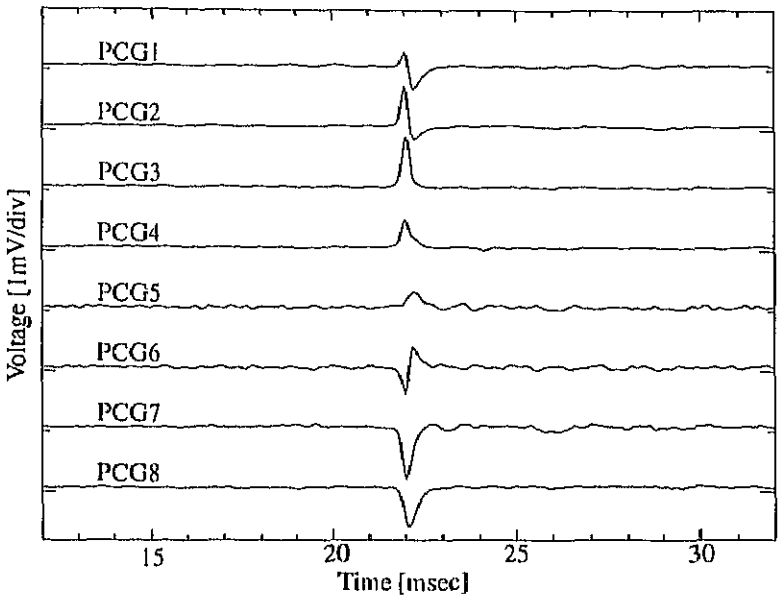

Fig. 2.20: Example of the pickup coil signals in high contact cable. The cable current was about 3100 A, and the quench heater used was HTD.

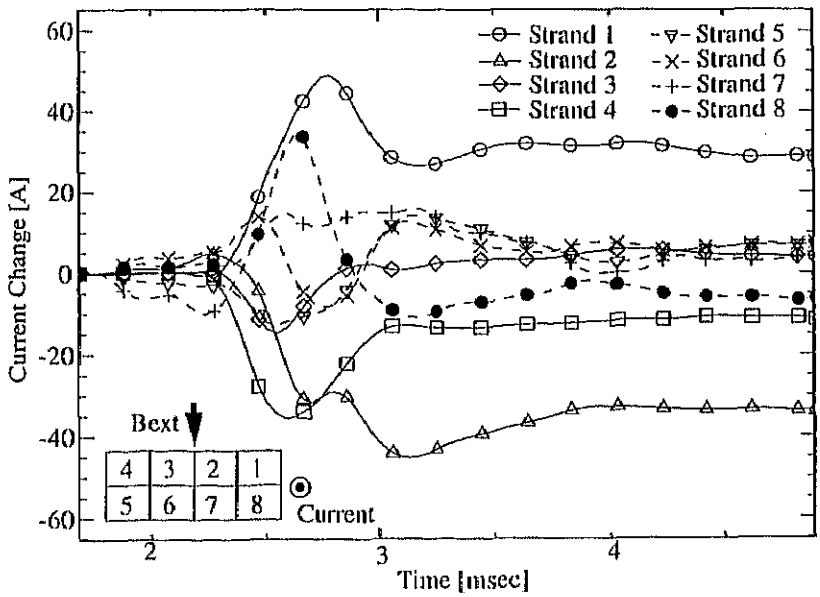

Fig. 2.21: Example of current changes of each strand calculated from the pickup coil signals of PCA in original cable at 3100 A.

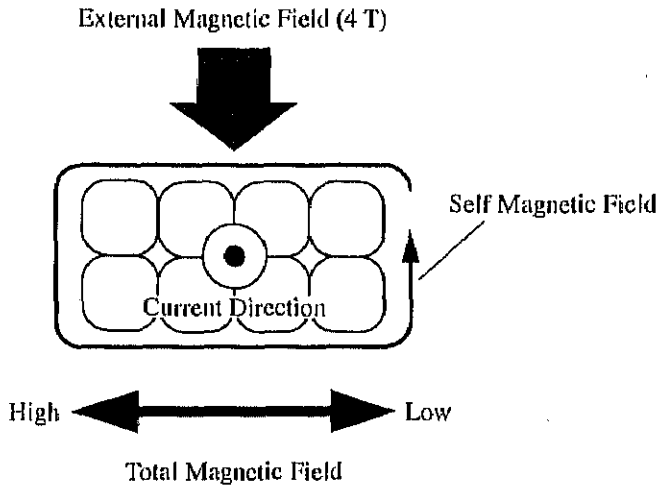

Fig. 2.22: Magnetic field applied to the cable.

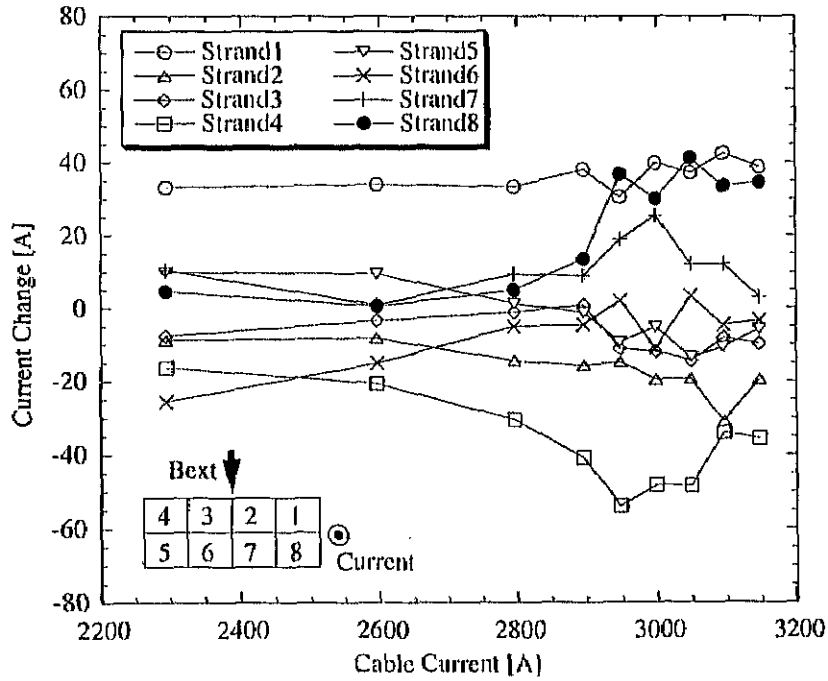

Fig. 2.23: Example of current changes of each strand in original cable at the time when the first current redistribution occurs.

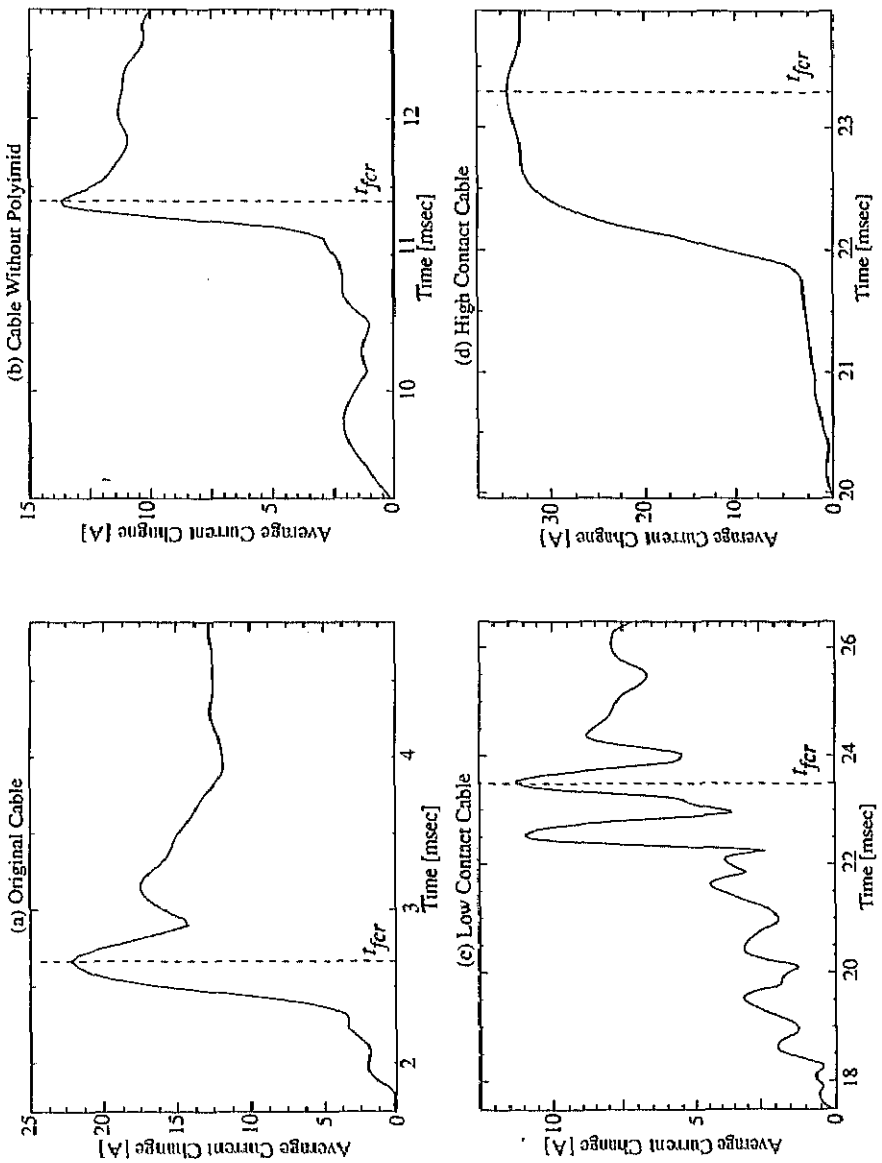

Fig. 2.24: Examples of average current changes for the four cables.

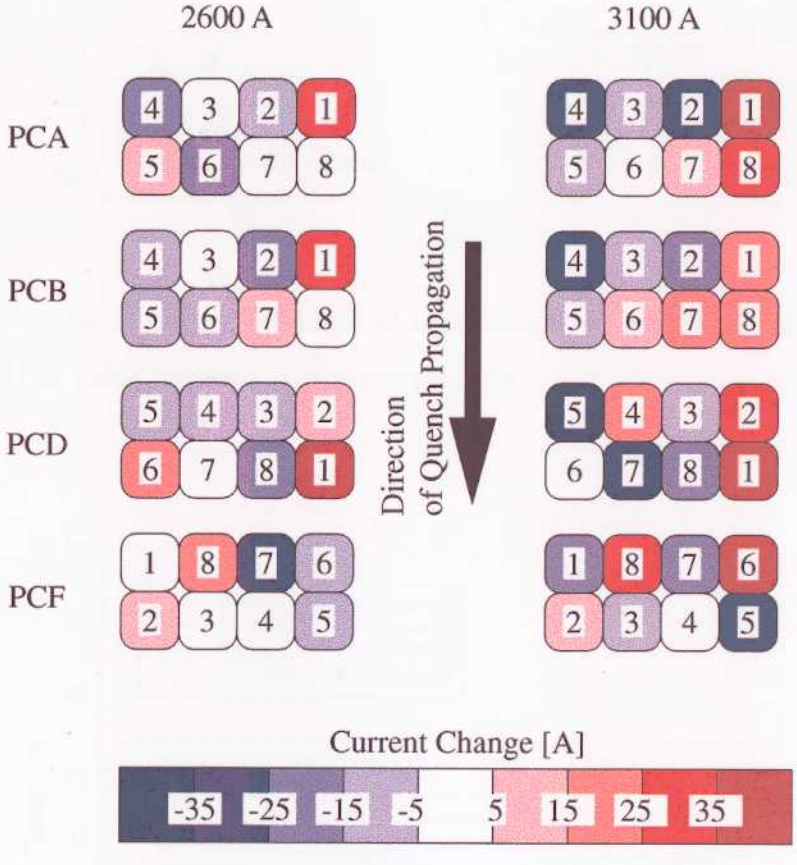

Fig. 2.25: First current redistributions at some longitudinal position in original cable. The amount of the current changes is distinguished by colors.

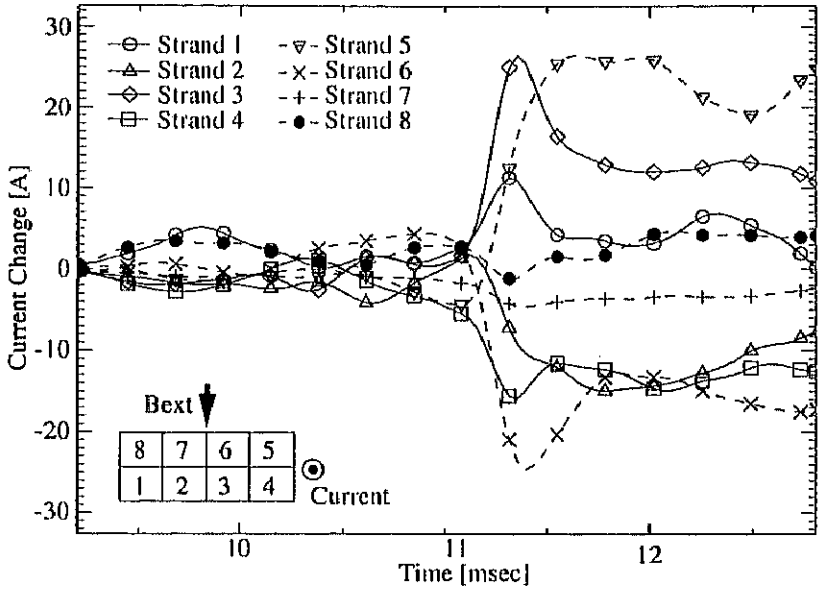

Fig. 2.26: Example of current changes of each strand calculated from the pickup coil signals of PCH in cable without polyimide at 3100 A.

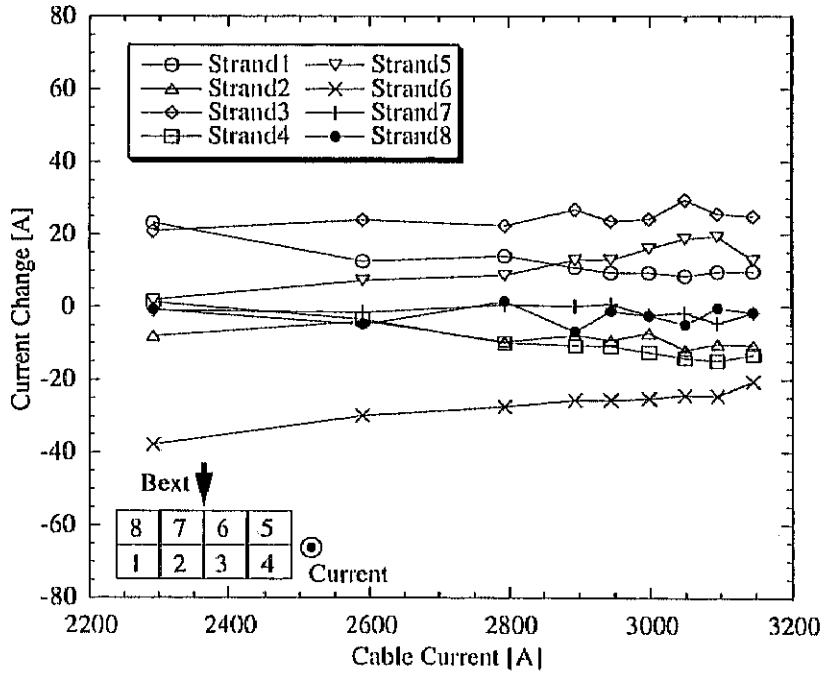

Fig. 2.27: Example of current changes of each strand in cable without polyimide at the time when the first current redistribution occurs.

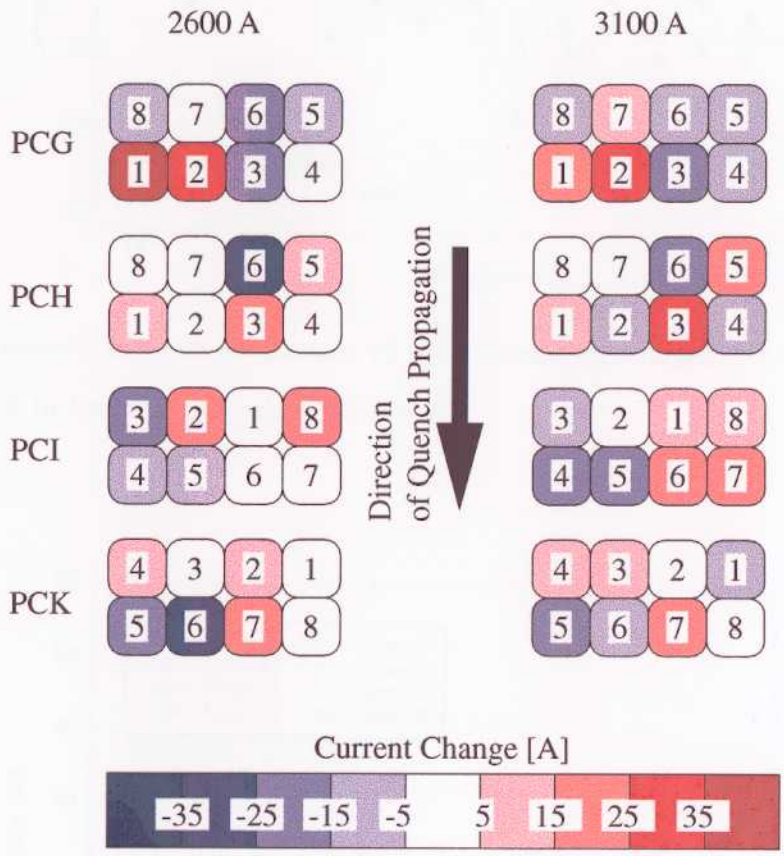

Fig. 2.28: First current redistributions at some longitudinal positions in cable without polyimide. The amount of the current changes is distinguished by colors.

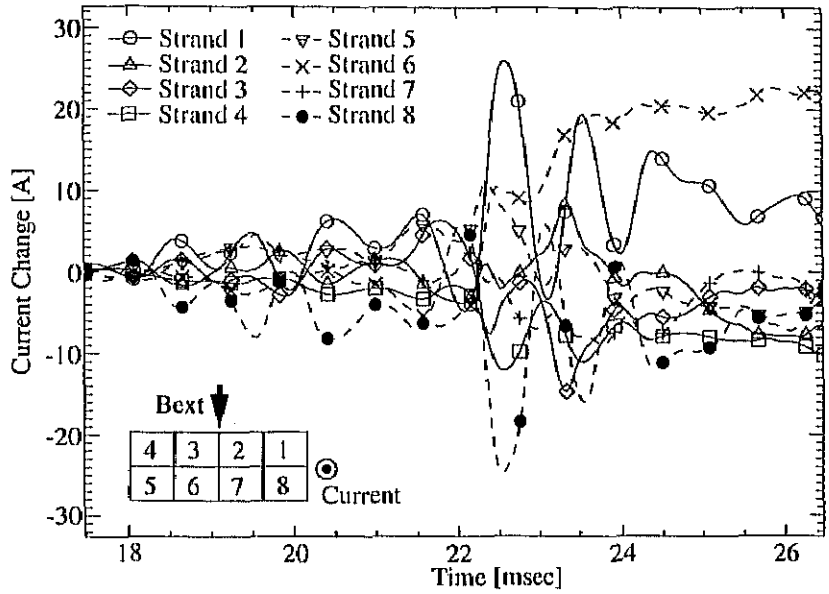

Fig. 2.29: Example of current changes of each strand calculated from the pickup coil signals of PCA in low contact cable at 3100 A.

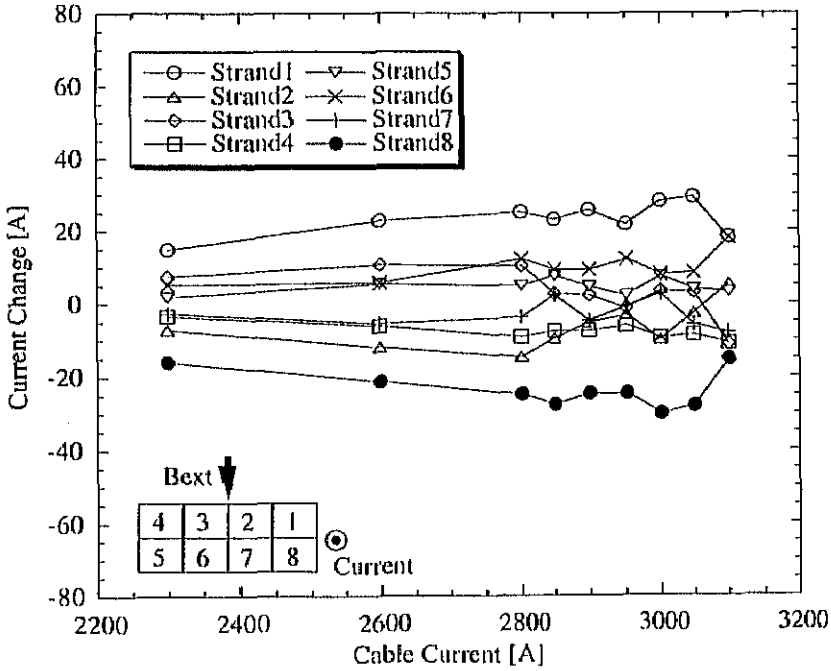

Fig. 2.30: Example of current changes of each strand in low contact cable at the time when the first current redistribution occurs.

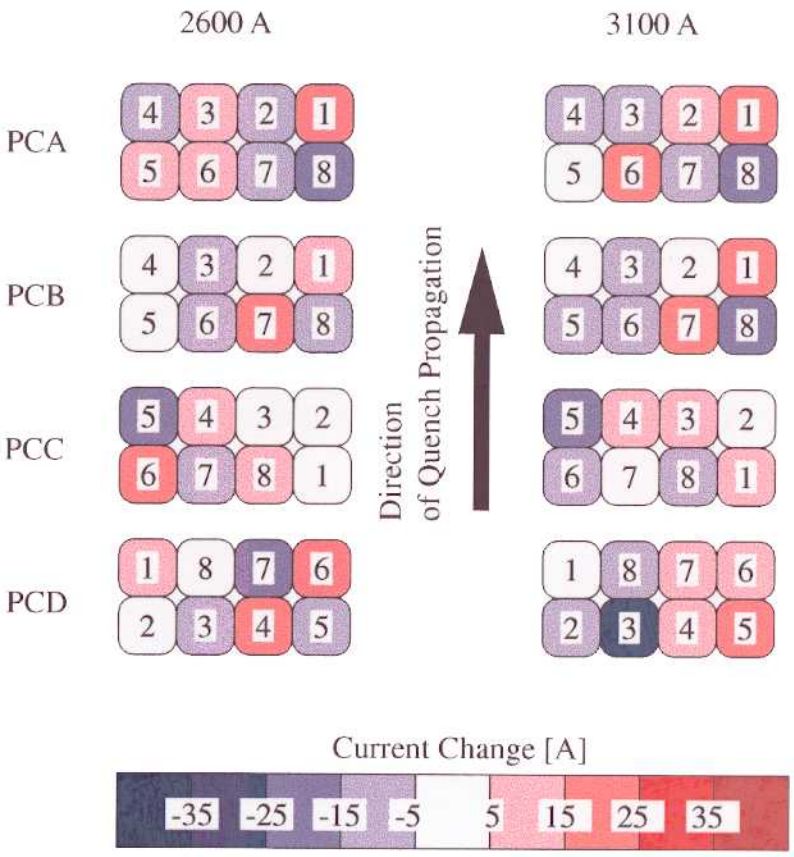

Fig. 2.31: The current redistribution at some longitudinal positions in low contact cable. The amount of the current changes is distinguished by colors. The quench heater is HTB.

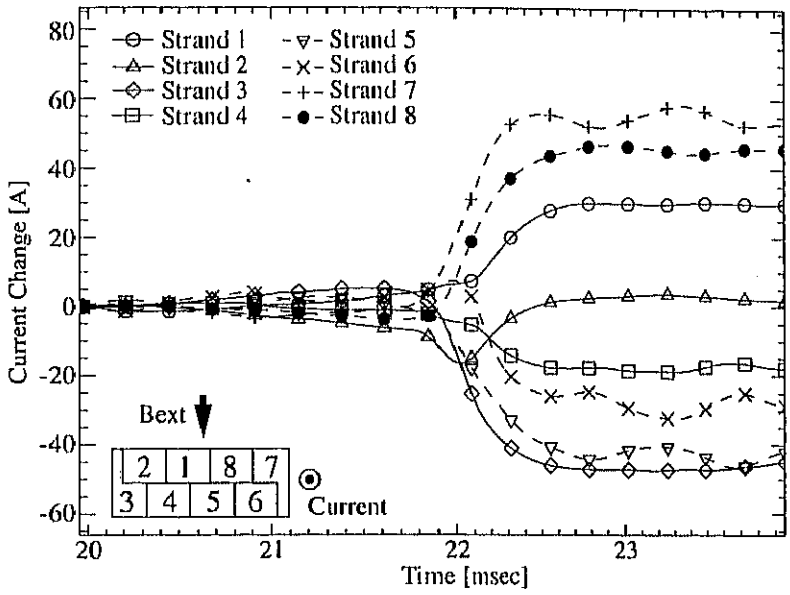

Fig. 2.32: Example of current changes of each strand calculated from the pickup coil signals in high contact cable at 3100 A. The set of pickup coils is PCG.

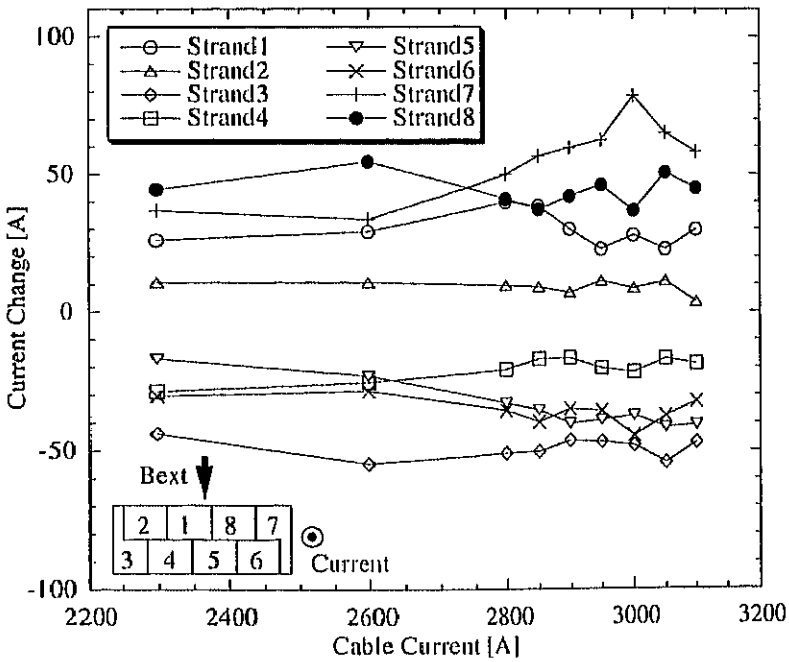

Fig. 2.33: Example of current changes of each strand at the first current redistribution in high contact cable. The set of pickup coils is PCG.

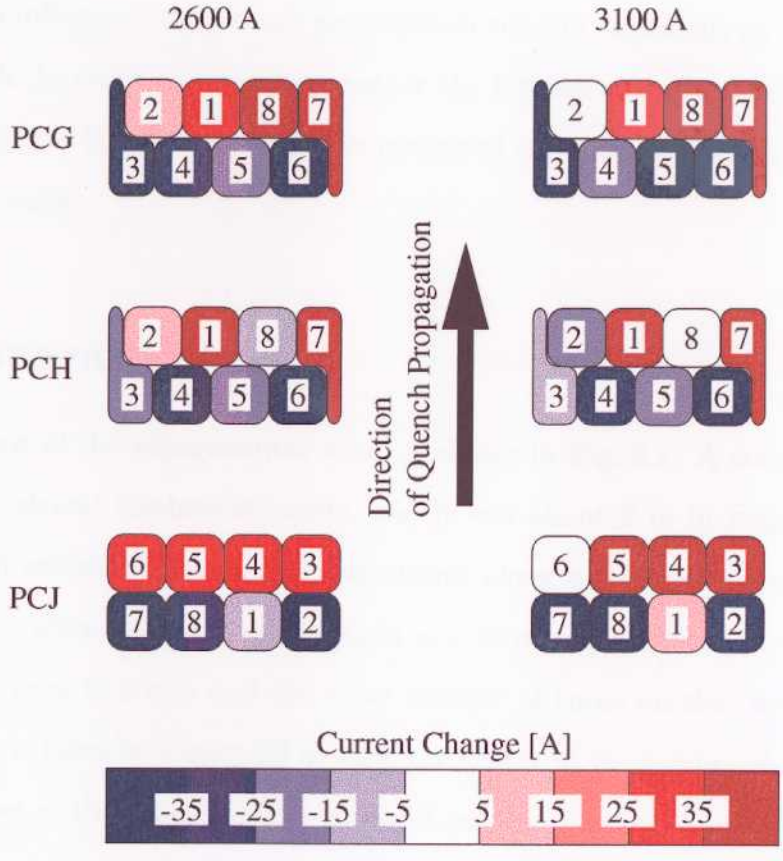

Fig. 2.34: The current redistribution at some longitudinal positions in high contact cable. The amount of the current changes is distinguished by colors. The quench heater is HTD.